Review Article - Narrative Review

Taiwan J Ophthalmol 2024;14:319-332

Access this article online

Quick Response Code:

Website: http://journals.lww.com/TJOP

DOI: 10.4103/tjo.TJO-D-24-00053

Artificial intelligence and big data integration in anterior segment imaging for glaucoma

Sunee Chansangpetch[1,2]*, Mantapond Ittarat[3], Wisit Cheungpasitporn[4], Shan C. Lin[5]

Abstract:

The integration of artificial intelligence (AI) and big data in anterior segment (AS) imaging represents a transformative approach to glaucoma diagnosis and management. This article explores various AS imaging techniques, such as AS optical coherence tomography, ultrasound biomicroscopy, and goniophotography, highlighting their roles in identifying angle-closure diseases. The review focuses on advancements in AI, including machine learning and deep learning, which enhance image analysis and automate complex processes in glaucoma care, and provides current evidence on the performance and clinical applications of these technologies. In addition, the article discusses the integration of big data, detailing its potential to revolutionize medical imaging by enabling comprehensive data analysis, fostering enhanced clinical decision-making, and facilitating personalized treatment strategies. In this article, we address the challenges of standardizing and integrating diverse data sets and suggest that future collaborations and technological advancements could substantially improve the management and research of glaucoma. This synthesis of current evidence and new technologies emphasizes their clinical relevance, offering insights into their potential to change traditional approaches to glaucoma evaluation and care.

Keywords:

Anterior segment imaging, artificial intelligence, big data, data standardization system, glaucoma

[1]Department of Ophthalmology, Faculty of Medicine, Chulalongkorn University and King Chulalongkorn Memorial Hospital, Thai Red Cross Society, [2]Center of Excellence in Glaucoma, Chulalongkorn University, Bangkok, [3]Surin Hospital and Surin Medical Education Center, School of Ophthalmology, Suranaree University of Technology, Surin, Thailand, [4]Department of Medicine, Mayo Clinic, Rochester, MN, [5]Glaucoma Center of San Francisco, San Francisco, CA, USA

***Address for correspondence:**
Dr. Sunee Chansangpetch, Department of Ophthalmology, Faculty of Medicine, Chulalongkorn University and King Chulalongkorn Memorial Hospital, Thai Red Cross Society, 1873, Rama IV Road, Pathumwan, Bangkok 10330, Thailand.
E-mail: sunee.ch@chula.ac.th

Submission: 13-05-2024
Accepted: 19-06-2024
Published: 13-09-2024

Introduction

Anterior segment (AS) imaging includes various techniques used to visualize and evaluate the front part of the eye. In glaucoma, these techniques provide both qualitative and quantitative assessment of angle width, aiding in the detection and management of angle-closure disease. In addition, they offer detailed views from different angles, revealing the anatomical relationships within AS structures and providing deeper insights into the mechanisms of angle closure. Emerging artificial intelligence (AI) technologies have shown significant potential in image analysis, offering the ability to learn from data and improve autonomously, thus providing a more adaptable and efficient approach to AS image analysis. AI technologies have proven their effectiveness in various aspects of glaucoma care, including angle parameter quantification, angle-closure detection, angle grading, differentiation of angle-closure mechanism subtypes, peripheral anterior synechiae (PAS) detection, and predicting treatment outcomes. This review aims to explore various AS imaging techniques, highlighting their roles in glaucoma management and presenting the latest advancements in AI that enhance image analysis and automate complex processes in glaucoma care. It also discusses the clinical applications of these technologies and the potential integration of big data in AS imaging.

Anterior Segment Imaging in Glaucoma

AS imaging encompasses various techniques used to visualize and evaluate the front part of the eye, including the cornea, iris,

How to cite this article: Chansangpetch S, Ittarat M, Cheungpasitporn W, Lin SC. Artificial intelligence and big data integration in anterior segment imaging for glaucoma. Taiwan J Ophthalmol 2024;14:319-32.

lens, and anterior chamber. Some of the most common techniques of AS imaging include slit-lamp photography, AS optical coherence tomography (AS-OCT), ultrasound biomicroscopy (UBM), and goniophotography.

In glaucoma, AS imaging mostly serves as a diagnostic tool to aid in the detection and management of angle-closure disease. This spectrum of ocular conditions, which includes primary angle-closure suspect (PACS), primary angle-closure, and primary angle-closure glaucoma (PACG), poses a significant global health challenge. Angle-closure glaucoma (ACG) is a more severe form of glaucoma compared to its open-angle counterpart. Despite constituting only 24% of primary glaucoma cases, ACG is responsible for nearly half of the bilateral blindness caused by glaucoma worldwide.[1] The projected increase in the prevalence of ACG–to 23.36 million by 2020 and 32.04 million by 2040–underscores the need for effective diagnostic strategies for early detection.[2] Differentiating between open-angle glaucoma and ACG is essential for the identification of individuals at risk and the implementation of appropriate management strategies. Traditional angle assessment methods like gonioscopy have been a gold standard method for evaluating angle anatomy, but the inherent subjectivity and variability in gonioscopy have raised concerns about its accuracy and consistency. In addition, the technical challenges and the requirement for an experienced ophthalmologist to perform the procedure limit its widespread use.[3,4]

Cross-sectional imaging tools such as AS-OCT and UBM provide an objective evaluation of angle width. The quantitative parameters from these devices have been extensively used in the literature to both identify and quantitatively assess the risk of angle closure.[5-7] These parameters are designed to capture the anatomical features of the AS, including the angle, iris, lens, ciliary body, and anterior chamber. The definitions of angle parameters typically involve certain distances (e.g. 250 μm, 500 μm, and 750 μm) from the scleral spur.[8] The parameters such as angle opening distance (AOD), angle recess area (ARA), trabecular iris space area (TISA), and trabecular iris angle (TIA) quantify the openness of the anterior chamber angle, measuring it in terms of linear distance (AOD), area (ARA, TISA), and angular degrees (TIA). The anterior chamber depth (ACD) and anterior chamber width (ACW) delineate the anterior chamber's dimensions. The lens vault (LV) metric describes the extension to which the lens protrudes into the anterior chamber, and iris thickness (IT) gauges the thickness of the peripheral iris. Further, distances such as iris-ciliary process distance, iris-lens contact distance, and trabecular-ciliary process distance elucidate the spatial relationships between the structures of the posterior chamber.[3]

In addition to quantitative assessment, AS-OCT and UBM provide detailed views from different angles, revealing the anatomical relationships within the AS structures and leading to deeper insights into the mechanisms of angle closure. The condition can be classified morphologically into pupillary and nonpupillary block mechanisms. Pupillary block is the primary mechanism, occurring in both primary and secondary ACG. It involves a resistance to the flow of aqueous humor from the posterior to the anterior chamber through the pupil, creating a pressure gradient that pushes the iris forward to obstruct the trabecular meshwork. Nonpupillary block mechanisms, specific to primary ACG, include plateau iris characterized by a steep iris root and a flat central iris plane due to anterior rotation of the ciliary body, thick peripheral iris with significant circumferential folds, and high LV where the anterior portion of the lens protrudes into the anterior chamber.[9] These imaging techniques are instrumental in assessing these morphological characteristics that contribute to angle closure.

AS imaging techniques such as AS-OCT and UBM can also help in evaluating and monitoring the efficacy of treatments like laser peripheral iridotomy (LPI). They can effectively visualize the results of LPI or argon laser peripheral iridoplasty by assessing the opening of the angle or the patency of the iridotomy. In addition, for procedures such as trabeculectomy, slit-lamp photography provides a clear view of the bleb's external appearance, while AS-OCT offers complementary insights into the internal morphology of the bleb, enhancing the overall monitoring and evaluation of treatment outcomes.

Ultrasound biomicroscopy

UBM utilizes high-frequency transducers to create images of the AS, offering resolutions between 20 and 60 μm and a depth of tissue penetration of approximately 4–5 mm. This method is especially valuable for visualizing dynamic changes within the eye, such as the light-dark response, and for imaging structures located posterior to the iris that were previously difficult to examine with standard clinical methods. The real-time, cross-sectional images produced by UBM can assess various ocular conditions, although the technique's efficacy can be influenced by the examiner's technique and experience.

Optical coherence tomography

OCT uses low-coherence interferometry to produce static cross-sectional images of ocular tissues. The AS-OCT is specifically tailored for imaging the front part of the eye, employing a laser wavelength of 1300–1310 nm for enhanced penetration through nontransparent tissues like the sclera. This differs from conventional OCT used for the posterior segment, which operates at wavelengths

of 830–880 nm. Notably, many posterior segment OCT devices now incorporate an AS module, often through a lens adaptor, to focus on the AS. OCT is known for its rapid, noncontact image acquisition, enabling the display of images in both cross-sectional views of individual angles and whole AS views. Several AS-OCT devices are currently available on the market, including the Visante OCT (Carl Zeiss Meditec, Dublin, CA, USA), which operates on time-domain OCT technology, and devices such as the CASIA SS-100 and its successor, the CASIA2 (Tomey, Inc., Nagoya, Japan), as well as the Anterion (Heidelberg Engineering, Heidelberg, Germany), which utilize swept-source OCT technology.

Goniophotography

Goniophotography is an imaging technique that captures an image view similar to gonioscopy, allowing for the visual assessment of the eye's anterior chamber angle. Some devices can be operated by a trained technician. An automated goniophotography device, Gonioscope GS-1 (Nidek, Gamagori, Japan), uses a 16-face multi-mirror optical gonioprism and a built-in image sensor to provide a comprehensive 360° view of the iridocorneal angle, which can be recorded in one examination. On the other hand, wide-field digital retinal imaging devices such as RetCam (Clarity Medical Systems, Inc., Pleasanton, CA, USA) and EyeCam (Clarity Medical Systems, Pleasanton, CA, USA), conventionally used for retinal imaging, have been adapted for goniophotography by addition of a 130° wide-field lens.[10,11] Modifications allow them to capture wide-field images of the iridocorneal angle in a supine position.

Artificial Intelligence and Image Analysis

Traditional programming methods in image analysis operate on a predefined set of rules tailored for specific applications. However, their rule-based nature means they are designed for particular scenarios and may not generalize well across varying conditions, which can limit their adaptability. The development of these traditional methods, while not requiring extensive datasets, tends to be time-consuming and labor-intensive due to the need for manual rule-setting and rigorous testing. This limitation has prompted the shift toward more innovative AI methods such as machine learning (ML) and deep learning (DL). These advanced techniques have demonstrated significant potential in image analysis, offering the ability to learn from data and improve autonomously, thereby providing a more adaptable and efficient approach to image analysis.

AI is a part of computer science that essentially exhibits intelligent behavior in a way that mimics human cognition. This involves several facets, including the capacity for reasoning, learning, and adapting through experiences, communicating in natural language, and even displaying lifelike behaviors. Techniques employed in AI range from logical reasoning and learning algorithms to language processing and robotics, all aimed at enabling machines to perform tasks that typically require human intelligence.[12]

ML, a subset of AI, enables machines to glean knowledge from data, drawing inferences and making predictions.[12-14] It comprises both supervised learning, which uses labeled data to forecast specific outcomes, and unsupervised learning, which is adept at discovering hidden patterns within datasets. DL, a specialized branch of ML, is characterized by its use of multiple layers within artificial neural networks. This architecture empowers machines to learn with greater depth from larger or more intricate datasets, yielding more precise inferences. In image analysis, traditional ML algorithms such as support vector machines usually require manual feature extraction by human experts, a process where specific attributes are chosen from raw data to perform a task like detecting pathologies in medical scans. It entails stages of data input, feature extraction, classification, and output, requiring manual intervention to identify relevant features.[12] However, the advent of DL, particularly convolutional neural networks (CNNs), streamlines this process by inputting data and outputting analyses directly. DL features are automatically tailored to specific tasks, eliminating the need for human intervention in this phase. Unlike handcrafted features, learned features in DL are complex and task-specific, refined through a process known as back-propagation.[12] This iterative feedback loop continuously improves the precision of the algorithm's outputs. In general, the workflows of ML and DL involve preparing data, partitioning datasets, creating model optimization, and performing system evaluation. The process commences with preprocessing images, dataset partitioning into training, validation, and testing datasets, and concludes with model selection and evaluation against statistical metrics and benchmarks.[14]

In the medical field, image analysis involves processing and interpreting visual information to extract meaningful insights. The process starts with the input of an image, which then undergoes a series of analysis steps, such as quality control or enhancement, to improve the image's clarity and usability. Localization techniques are applied to identify and isolate areas of interest within the image. The process then transitions to extracting clinically relevant information, tailored to the objective of the analysis.[15,16]

AI has the capacity to manage and interpret vast amounts of data with precision and speed. Once an image is input into the system, AI can perform tasks like quality

control and enhancement to ensure that the image is of the highest possible clarity and usability. For instance, AI can augment, convert, or equalize images to improve their utility.[16] After the initial enhancement, AI can assist in localizing specific regions within the image that are of interest, a process often followed by segmentation to isolate and study these areas in detail.[17] AI can also select the region of interest (ROI) and identify structural elements within the image. Quantification is another step where AI measures and calculates the attributes of the localized features, leading to more precise and objective analysis. The analysis may include various clinical parameters that AI tools help to identify as relevant. For clinical applications, the processed data can feed into tasks such as diagnosis, prediction, classification, and prognostication, significantly improving the efficiency of medical assessments. In the end, the output of the image analysis process is a comprehensive synthesis of all the previous steps, delivering results that can be directly utilized in clinical settings or further research. Figure 1 summarizes the image analysis process with examples of AI-assisted tasks. This overview not only highlights the capabilities of AI in handling complex datasets but also its transformative potential in advancing medical imaging and analysis.

Analyzing Anterior Segment Imaging

Image quality

The first step in the workflow involves image preprocessing, which is vital for setting a strong foundation for further analysis. This stage generally involves reducing noise in the images, such as eliminating specular reflections commonly found in ocular images, removing uneven illumination and artifacts that could hide critical details, and performing tasks such as augmentation, conversion, equalization, and enhancing resolution. Many of these tasks can be effectively supported by AI algorithms.

Several studies have utilized AI-assisted techniques to assess or improve image quality in AS imaging. Niwas *et al*. proposed an automated quality assessment of AS-OCT images using a Naïve Bayes classifier to produce a quantitative quality index.[18] The classifier's performance was validated against expert assessments, achieving an overall accuracy of 82.9%. This ML approach enables objective evaluation of AS-OCT image quality, aligning closely with clinical expert evaluations.

Ouyang *et al*. addressed both speckle noise and imaging artifacts, such as shadowing and specularity, which typically hinder the analysis of AS structures in OCT images.[19] They proposed a cascaded neural network framework, combining a conditional generative adversarial network (cGAN) with a tissue interface segmentation network. This hybrid approach showed high accuracy in segmenting tissues. This study represents the first to integrate a cGAN within larger DL frameworks for enhanced segmentation of OCT images, improving both visualization and performance of segmentation algorithms.

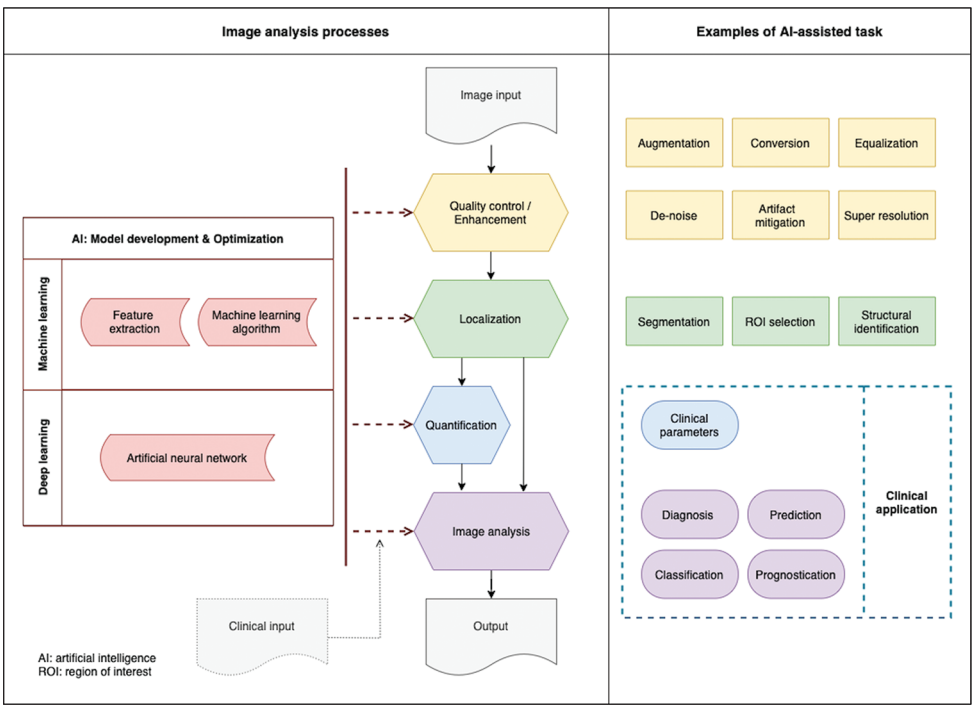

Figure 1: A framework for artificial intelligence-assisted tasks in image analysis. AI = Artificial intelligence, ROI = Region of interest

For noise reduction, Liu *et al*. introduced a CNN-based denoising algorithm specifically designed to tackle speckle noise, which is prevalent in OCT images of the AS.[20] The approach learns the speckle noise distribution using a trainable OCT dataset to indirectly produce the denoized images. Remarkably, the algorithm preserved essential details and textures while maintaining strong edge preservation capabilities. It also processed images within 0.4 s, enabling practical clinical application.

More recently, Li *et al*. introduced an advanced generative AI technique using a DL-based diffusion model to enhance AS-OCT images, termed the Content-Preserving Diffusion Model.[21] This unsupervised model significantly reduces speckle noise and transforms it into a Gaussian distribution through a reverse diffusion process. This approach preserves the inherent content of images while removing noise, which further facilitates better performance in segmentation and localization tasks.

Localization

The next step is to locate the area of interest based on the purpose of the analysis.

Localization involves pinpointing specific areas within an image where key features or objects (e.g. the iridocorneal angle) are located. Segmentation further aids by dividing the image into meaningful regions, isolating these critical features from the broader image. For instance, in angle analysis, segmentation can precisely delineate the boundaries of the anterior chamber angle, cornea, iris, ciliary body, and lens, which are vital for understanding the factors contributing to angle-closure pathogenesis.

For ML, localization and segmentation are preparatory steps that facilitate feature extraction, ROI selection, and further analysis. Relevant features are selected and extracted to facilitate efficient learning and to increase the model's accuracy. DL, by contrast, can often handle raw images without the need for extensive feature engineering due to the capability of layers within CNNs to automatically extract and learn the best features for classification tasks.

Anatomical identification or annotation not only serves as the initial stages of algorithm development but also holds significant clinical value. Measuring clinical parameters often relies on identifying reference landmarks. For instance, quantifying angle parameters typically depends on the location of the scleral spur, and less frequently on Schwalbe's line.[22,23] The identification of other angle structures, such as Schlemm's canal and collector channels, is important for evaluating the conventional outflow pathway. In addition, segmenting structures such as the iris, lens, and ciliary body enables the quantitative and qualitative assessment of morphological characteristics that contribute to angle closure.[24-26] These tasks can be assisted by AI.

Scleral spur detection

The most common reference location in anterior chamber evaluation is the scleral spur. Several studies have developed DL algorithms for automating scleral spur detection in UBM,[27-29] and AS-OCT with Visante,[30] CASIA1000,[24,31] CASIA2,[32] and the Anterion,[33] as shown in Figure 2. The Euclidean distance error, which reflects the accuracy of annotation, is relatively small overall. The range of errors for all angle statuses is 43–77 μm, for an open angle of 66–87 μm; and for a closed angle, it extends from 84 to 134 μm. Internal validations generally show lower errors than external validations, which is expected. In closed angles, there

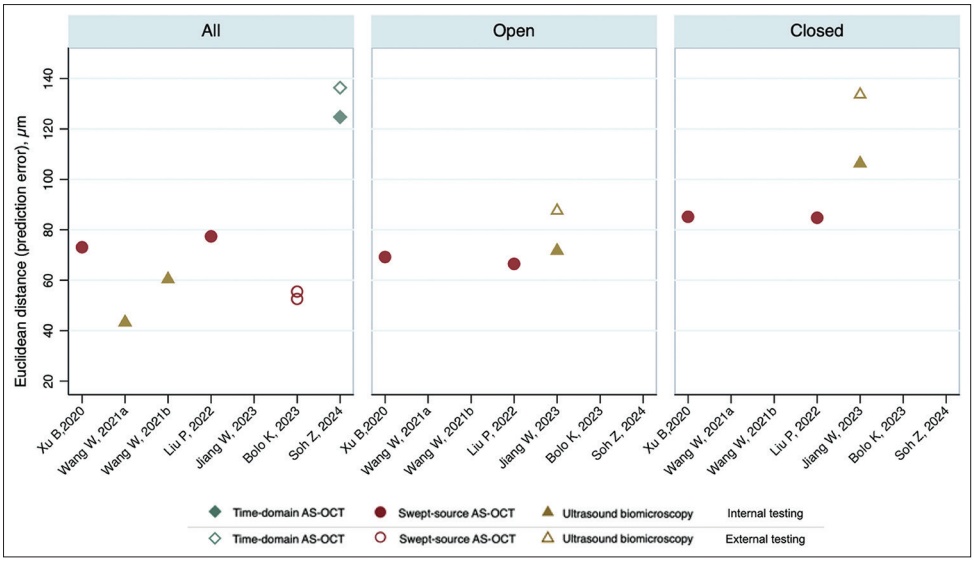

Figure 2: Accuracy in scleral spur identification across studies. AS-OCT = Anterior segment optical coherence tomography

is a noticeable increase in the error rates, which might suggest that closed angle status is still more challenging for DL algorithms to annotate accurately.

Aqueous humor outflow mapping

Huang *et al*. described ML algorithms to map the aqueous humor outflow (AHO) system from spectral-domain (SD)-OCT images, enabling the three-dimensional (3D) reconstruction of the AHO system, particularly focusing on Schlemm's canal and collector channels.[34] The techniques involved a Bayesian Ridge method for initial location approximation and a fuzzy hidden Markov model for the segmentation tasks. These approaches allowed for the identification and visualization of the AHO structures, offering potential enhancements in personalized surgical interventions and in understanding glaucoma pathogenesis.

Goniophotography

Goniophotography offers an alternative approach to assessing the angle, providing some advantages over traditional gonioscopy. While AS cross-sectional imaging techniques such as AS-OCT and UBM have constraints in directly examining the surface of the anterior chamber angle, which impacts the ability to detect key observations such as angle neovascularization, trabecular meshwork pigmentation, or PAS. Given these limitations, goniophotography offers a useful alternative, potentially providing an enhanced visualization of these pathological features.

Peroni *et al*. developed a DL model to perform segmentation (specifically of the ciliary body band, scleral spur, trabecular meshwork, and cornea) and ROI identification from goniophotographs.[35] The model achieved a segmentation accuracy of about 91%, successfully identifying appropriate ROIs in all test frames and pinpointing errors in segmentation outputs.

However, there is scant research thus far on the use of ML or DL to analyze goniophotography, especially in detecting pathological lesions. Future studies are necessary to develop models that are specifically tailored to effectively recognize these lesions, using large, targeted datasets.

Clinical application

Quantification: Clinical parameters

Even though gonioscopy is the current gold standard for angle evaluation, it is subjective and shows variable reproducibility.[3] Quantitative OCT-based methods could enhance the assessment of the anterior chamber angle, providing a reliable complement to gonioscopy. Recently, DL algorithms have shown promise in accurately quantifying AS parameters from various imaging modalities.[28-30,33,36,37]

Soh *et al*. developed a DL algorithm that automates the measurement of angle width parameters from Visante OCT images.[30] The intraclass correlation coefficients (ICC) for the angle measurements (i.e. AOD500, AOD 750, TISA500, TISA750) varied from 0.71 to 0.87, reflecting good reliability. The study also reported ICCs for iris and anterior chamber parameters, with ICCs ranging from 0.54 to 0.99. Subgroup analysis showed comparable ICCs between open-angle and closed-angle subgroups.

Wang *et al*. and Jiang *et al*. focused on UBM images, developing DL systems that quantitatively measure angle parameters with a high degree of accuracy.[28,29] Wang *et al*.'s study reported small mean differences between automated and manual measurements, with coefficients of variation for various angle parameters such as TIA500 and AOD750 ranging from 4.67% to 16.77%. Jiang *et al*.'s findings showed small average relative errors for angle parameters under 15% and ICCs for all angle-related and IT parameters exceeding 0.88.

Bolo *et al*. performed external testing of a built-in DL algorithm on Anterion AS-OCT, focusing on scleral spur-based biometric parameters.[33] Their study reported ICCs from 0.946 to 0.994 for various superior angle parameters. Temporal angle parameters and other metrics like LV and ACW also showed high ICCs, supporting the high performance of the DL algorithms in different settings. Table 1 summarizes the mean difference between the automated and manual measurements of common angle parameters across different studies.

Table 1: Mean difference between the automated deep learning and manual measurements of common angle parameters

Study	Device	Testing type	AOD500 (mm)	AOD750 (mm)	TISA500 (mm^2)	TISA750 (mm^2)	ARA500 (mm^2)	ARA750 (mm^2)	TIA500 (°)
Wang W, 2021	UBM	Internal	0.0012	0.0056	N/A	N/A	−0.003	−0.005	0.370
Bolo K, 2022	Anterion	External	−0.0150	N/A	−0.006	N/A	N/A	N/A	N/A
Jiang W, 2023	UBM	Internal	0.0096	0.0137	0.004	0.007	0.008	0.011	0.708
		External	0.0219	0.0282	0.008	0.182	0.019	0.024	1.675
Soh Z, 2024	Visante	Internal	0.0100	0.0100	0.000	0.000	N/A	N/A	N/A

AOD=Angle opening distance, TISA=Trabecular-iris space area, ARA=Angle recess area, TIA=Trabecular iris angle, UBM=Ultrasound biomicroscopy, N/A=Not available

Although studies indicate that DL algorithms are highly effective, with strong correlation and minimal error in measuring angle parameters, there may be some skepticism regarding the use of these parameters as features in diagnosing angle closure. A study by Fu *et al*. highlighted that a DL system outperformed a traditional ML approach, which utilized a quantitative feature-based system in detecting angle closure.[36] The DL system demonstrated a superior area under the receiver operating characteristic curve (AUC), sensitivity, and specificity in identifying angle-closure conditions.

While DL shows promise in more accurately classifying angle closure than traditional quantitative methods, these quantitative measures still hold significant value in the clinical management of angle closure. They are clinically interpretable, serve as key parameters for monitoring disease progression, and may be more appropriate for some research settings. Moreover, specific parameters such as AOD and TISA have been demonstrated to play a significant role in predicting the progression of primary angle closure disease (PACD) and in assessing the response to treatments like LPI.[38-40] In addition, they are easier to communicate to patients during educational interactions, unlike the more complex outputs of DL, which can be challenging to explain.

Angle-closure detection

The existing literature on the application of ML and DL in detecting angle closure from AS imaging presents a continuously evolving field. Figure 3 compiles studies using AS-OCT and UBM imaging techniques.[23,28,29,36,41-52] This plot, covering research from 2012 to 2023, illustrates a progression toward enhanced diagnostic accuracy.[23,28,29,36,41-52] AS-OCT, including time-domain, SD, and swept-source, along with UBM, has been employed to various extents, yielding AUCs between 0.84 and 0.98 for ML,[23,41,42,52] and 0.85 to nearly 1.00 for DL approaches[28,29,43-51] [Figure 3].

The initial stage of automating angle-closure detection involved using ML algorithms to analyze visual features extracted from AS images. These features were either used independently,[41,42] or combined with clinical parameters.[23] In general, visual features, which offer more detailed information compared to clinical parameters, produced superior outcomes in determining angle status.[41,42] The process of feature selection usually focused on identifying critical anatomical landmarks, though occasionally it employed shape analysis.[23]

Learned features from DL algorithms may include image information that extends beyond what clinicians typically consider important for detecting angle closure, compared to manually extracted features from ML algorithms. The reported DL algorithms tend to

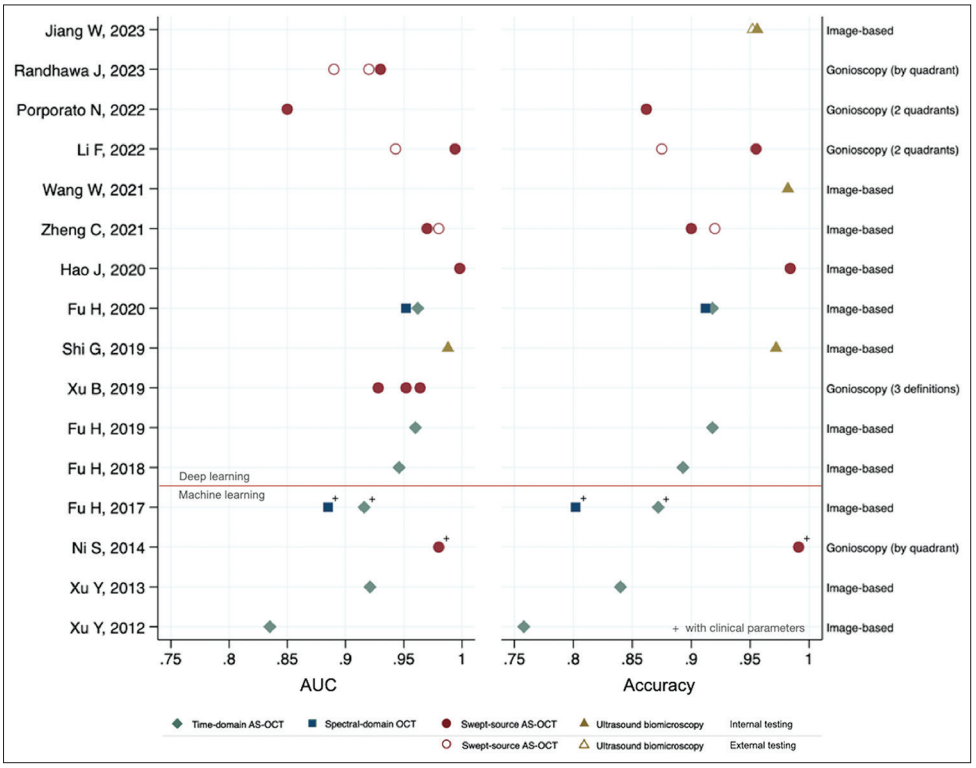

Figure 3: Machine learning and deep learning performance in detecting angle closure using anterior segment imaging-the Y-axis on the left side of the plot lists the different studies by first author and publication year. The Y-axis on the right side categorizes the criteria used for angle closure in each study. AUC = Area under the receiver operating characteristic curve, AS-OCT = Anterior segment optical coherence tomography

yield higher performance in detecting PACD than the ML algorithms. However, DL effectiveness is often limited by the need for large, annotated datasets. Addressing this challenge, Zheng *et al*. utilized generative AI through semi-supervised generative adversarial networks (GANs).[47] The approach generates synthetic AS-OCT images to enrich the training dataset, overcoming data scarcity and enhancing diagnostic precision without extensive manual labeling.

More recent studies, particularly from 2021 onwards, have included external testing of the algorithms on independent datasets, which also show high performance, suggesting robustness in algorithm performance.[46-49] The criteria for angle-closure detection predominantly rely on image-based assessments, with some literature integrating gonioscopy measurements. The outcomes from algorithms based on gonioscopy criteria demonstrate more variability than those relying on image-based methods, potentially due to differences in gonioscopy definition and the intrinsic variability in performing gonioscopy. In addition, comparisons between different algorithms remain challenging due to variations in study samples and equipment used.

Several studies have developed models based on goniophotography for detecting angle closure. The early work by Cheng *et al*. employed ML techniques to automate the detection of angle closure from RetCam images.[53] Their automated analysis focused on detecting and outlining focal edges associated with angle structures. Baskaran *et al*. later assessed the performance of this automated grading, finding good agreement with gonioscopy for diagnosing angle closure when two or more quadrants were closed ($\kappa = 0.74$).[54] The AUC for detecting eyes with gonioscopic angle closure was 0.954, comparable to manual grading.

Building on this, Chiang *et al*. advanced the field by training a CNN classifier using the Residual Network (ResNet) architecture on EyeCam images to detect angle closure.[55] Their study demonstrated that the CNN achieved excellent performance, with a kappa of 0.746 and an AUC of 0.969, surpassing non-reference human graders.

Hao *et al*. utilized AS-OCT videos to study iris movements in real-time across changing lighting conditions, providing a dynamic view of iris behavior and anterior chamber changes that enable monitoring of physiological responses such as pupil dilation and constriction.[56] Changes in iris area and volume have been reported to be associated with ACG.[57] To improve the identification of angle-closure conditions, they developed a DL algorithm that leverages AS-OCT video datasets to automatically extract dynamic features for recognizing angle-closure eyes. This DL-based temporal classifier network incorporates ResNet and long short-term memory layers, proving highly effective in classifying angle closure with an AUC of 0.905.

Angle grading

AI demonstrates robust capabilities in classifying gonioscopic angle grades when employing both goniophotographs and AS-OCT images.

Based on goniophotographs, Zhou *et al*. used the Scheie grading system to develop a DL model, HahrNet, which achieved an accuracy of 96.18%, specificity of 99.04%, and sensitivity of 95.94%.[58] Chiang *et al*. employed a CNN based on the ResNetarchitecture to analyze EyeCam goniophotographs graded according to a modified Shaffer classification, achieving predictive accuracies of 97.5% for grade 0, 90.0% for grade 1, 65.5% for grade 2, 99.0% for grade 3, and 100% for grade 4.[55]

Using AS-OCT to compile gonioscopic grading scores presents more challenges compared to the straightforward nature of goniophotographs. Xu *et al*. applied the Shaffer grading system to swept-source AS-OCT images, documenting accuracies of 98.4% for grade 0, 89.1% for grade 1, 40.0% for grade 2, 87.4% for grade 3, and 98.9% for grade 4.[44] Notably, the accuracy for predicting images corresponding to grade 2 was nearly at chance levels, likely reflecting the low examiner certainty and the high dependence on dynamic examination gonio techniques. These gonioscopic techniques are difficult to accurately simulate or estimate in AI models, impacting the precision of predictions at this grade.

Differentiate subtypes of angle-closure mechanisms

Given that ACG encompasses various morphological mechanisms, each may respond differently to specific treatment modalities. Studies have leveraged various ML approaches to enhance the classification accuracy of ACG subtypes, including pupillary block, plateau iris, thick peripheral iris roll, and exaggerated LV. A study by Bai *et al*. implemented error-correcting output codes with optimized feature sets derived from AS-OCT images, achieving an 87.65% classification accuracy.[59] Similarly, Niwas *et al*. in 2015 utilized AdaBoost combined with principal component analysis for feature reduction, achieving a 74.85% accuracy. Their subsequent studies in 2016 further refined these approaches; one utilized an L-score feature selection to improve classifier power, reaching an 84.39% accuracy, while another introduced a novel feature extraction technique, achieving 89.20% accuracy.[60-62]

A more recent study by another group also utilized DL techniques for segmenting iris curvature to classify UBM images into iris bombe and non-iris bombe categories,

and for localizing the iris root to classify iris insertion into basal, middle, and apical categories.[29] Basal iris insertion refers to the iris root's location at the base of the ciliary body near the scleral spur and is a biometric risk factor for angle closure. The algorithms achieved accuracies of up to 94% in detecting iris bombe and 86% in classifying iris insertion. Another study focused on predicting plateau iris using DL techniques by Wanichwecharungruang *et al*., who developed algorithms to predict plateau iris from 716 images of AS-OCT quadrants.[63] All images were confirmed as plateau iris by their paired UBM images. The algorithm demonstrated high diagnostic performance with an AUC of 0.95, an accuracy of 94%, a sensitivity of 87.9%, and a specificity of 97.6%.

These collective efforts illustrate the capability of AI to distinguish between different ACG mechanisms, thereby aiding in facilitating better-targeted treatments. Nevertheless, one of the main limitations of using AI to differentiate subtypes of angle-closure mechanisms is the absence of a universally accepted "gold standard" for diagnosing these subtypes. This lack of standardized diagnostic criteria can lead to inconsistencies in training AI models. This limitation not only affects the reliability of AI diagnoses but also hampers the ability to effectively train and validate AI models on a large scale.

Peripheral anterior synechiae detection

Identifying and distinguishing between an appositional and synechial angle closure is crucial for clinicians to formulate an effective treatment plan in angle closure.[9] Gonioscopy, a gold standard angle examination, can detect PAS in synechial angle closure using a dynamic technique. However, both appositional and synechial angle closures often appear similar in static AS images. Efforts to use DL technology for detection have been explored.

Hao *et al*. developed a DL method that analyzes the spatial state of features across sequences of AS-OCT images rather than single images.[64] They conducted imaging under both dark and bright conditions to utilize changes in pupil size that mimic the pressure effects of goniolens. The work introduced a new metric, time-weighted cross-entropy loss, to capture both appearance and changes in appearance. This approach achieved an AUC of 0.844 in differentiating between appositional and synechial angle closures.

Similarly, Hao *et al*. utilized the changes between dark and light conditions captured by AS-OCT, and added 3D iris geometrical features to assess the AS-OCT images.[65] Their hybrid DL model, which combines two-dimensional and 3D data, achieved an accuracy of 0.829 in classifying open angle, appositional, and synechial angle closures, with an AUC of 0.859 for differentiating between appositional and synechial closures.

Furthermore, Li *et al*. developed an automated digital gonioscopy system using dynamic swept-source OCT examination under varying light conditions.[48] Their system, which analyzes paired light and dark data, demonstrated superior diagnostic performance, with an AUC of 0.885 at the clock-hour level and 0.902 at the quadrant level for detecting PAS.

Predicting treatment outcome

AI can also aid in predicting treatment outcomes. Koh *et al*. developed an automated algorithm employing ML techniques to predict the efficacy of LPI in treating eyes suspected of PACS using time-domain AS-OCT.[66] They defined success as the change of one or more angles from closed to open in AS-OCT scans after treatment. The algorithm utilized features such as correlation coefficients and the structural similarity index to predict outcomes. It achieved an accuracy of 89.7%, with a specificity of 95.2% and a sensitivity of 36.4%, based on pre-LPI AS-OCT scans only. This fully automated method aims to improve decision-making regarding prophylactic LPI for PACS by providing an objective evaluation of potential treatment success, thus optimizing patient selection and reducing unnecessary interventions.

Glaucoma surgery

The use of AI in evaluating glaucoma surgery outcomes is an emerging field, with limited studies developing ML and DL models for trabeculectomy evaluation. These studies analyze only slit-lamp photographs, in contrast to AI applications in detecting angle closure that often employ images from AS-OCT and UBM.

Wang *et al*. employed a Mask region-based CNN model to quantitatively assess the size of functional filtering blebs posttrabeculectomy.[67] Their study demonstrated that DL could effectively quantify bleb size, with all intersection over union scores exceeding 93%, indicating high accuracy compared to expert assessments. This suggests that DL could help standardize postsurgical evaluations, making them more objective and less reliant on subjective clinical judgments.

Expanding on this foundation, Mastropasqua *et al*. used ResNet architectures combined with ensemble learning techniques not only to assess physical dimensions but also to classify the overall functionality of blebs into three outcomes: complete success, qualified success, and failure. Their model achieved an AUC of 0.8, an accuracy of 74%, a sensitivity of 74%, and a specificity of 87%.[68]

The role of AI in glaucoma surgery is currently at an early stage of development. As the field stands, there

is substantial room for growth, particularly in areas such as predicting surgical outcomes and integrating data from various imaging modalities, including AS-OCT.

Anterior Segment Imaging and "Big Data"

"Big Data" is fundamentally characterized by its large-scale, complex data sets that traditional software struggles to process. The concept is characterized by the five versus: Volume, Velocity, Variety, Veracity, and Value. Volume addresses the massive amounts of data generated from various sources. Velocity refers to the rapid generation and movement of data. Variety involves the myriad types of data, from structured to unstructured. Veracity emphasizes the importance of data accuracy, with strategies in place to ensure reliability. Finally, value represents the core goal of big data analytics—to derive actionable insights for enhanced decision-making and outcomes.

Big data has the potential to greatly improve health care by enhancing patient outcomes, increasing operational efficiency, and accelerating medical research. The big data framework starts with varied data inputs – image, clinical, and others – each undergoing preprocessing to ensure quality and uniformity. These streams then converge in a data integration and standardization phase, essential for aligning disparate data formats into a singular analytical data frame. At the core of the process lies the data mining and analytics stage, where algorithms extract patterns from large data sets. These insights are then visually presented for easy interpretation, guiding the final decision-making process [Figure 4]. Across all these steps, AI can be instrumental in enhancing efficiency and accuracy throughout the entire process.

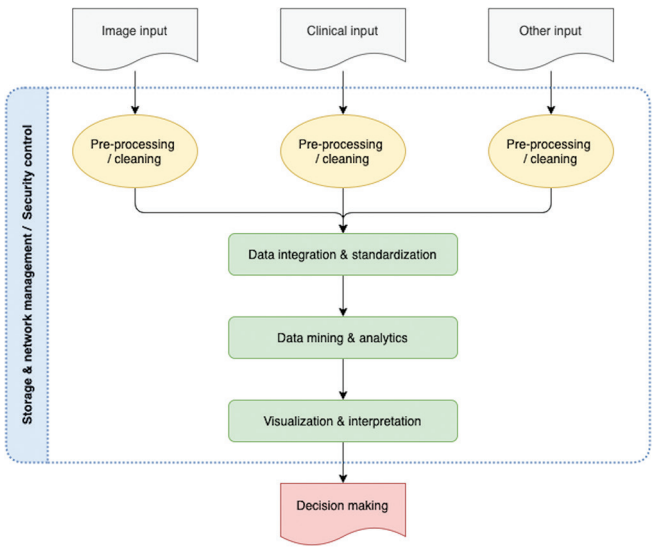

Figure 4: Framework for big data integration and analysis in decision-making

However, using images, including AS imaging, in big data frameworks poses significant challenges, mostly due to the complexity of analyzing unstructured image data that necessitates advanced algorithms for meaningful insights. Image quality and variability can significantly impact analysis accuracy. Furthermore, the interpretation of image data can be subjective, with inherent biases in collection and processing methods potentially leading to skewed results. Integrating image data with other types of data to perform comprehensive analyses also demands complex technical solutions, making it challenging to derive comprehensive insights from mixed data sources.

Currently, big data has not been directly utilized in AS imaging for glaucoma. However, the future integration of advanced AI tools, improved datasets, and collaborative efforts to establish data standardization systems could effectively promote the use of big data in this area. These advancements would enhance the analysis and utility of imaging data, potentially transforming management strategies and accelerating research in the glaucoma field [Figure 5].

Artificial intelligence tools

AI tools can be utilized across various stages of big data management. From preprocessing and data integration to analysis, visualization, and interpretation, AI enhances the capability to handle complex data efficiently. However, when it comes to specialized applications like AS imaging in glaucoma, there are significant challenges due to the absence of universally applicable, well-trained AI algorithms. This shortfall is primarily attributed to the lack of publicly available, labeled, valid, large, and diverse databases for AS imaging. This situation contrasts with the availability of fundus photography and optic nerve head imaging, where datasets such as the digital retinal images for vessel extraction,[69] retinal image database for optic nerve evaluation,[70] ORIGA database,[71] and REFUGE (Retinal Fundus Glaucoma Challenge) stand as exemplars of open-access resources.[72] The scarcity of high-quality, annotated data limit the potential for developing robust AI models for AS imaging that can reliably interpret such specific medical images across different patient demographics and conditions.

Generative AI is a subset of AI technologies that utilize various forms of existing data to learn and generate new content. Generative AI models, such as GANs, are capable of creating new, synthetic data samples that are realistic and varied. These models work by training two neural networks simultaneously–a generator that creates data and a discriminator that evaluates the data's authenticity. Through their iterative competition, these networks can produce high-quality, diverse datasets that mirror real-world variations.

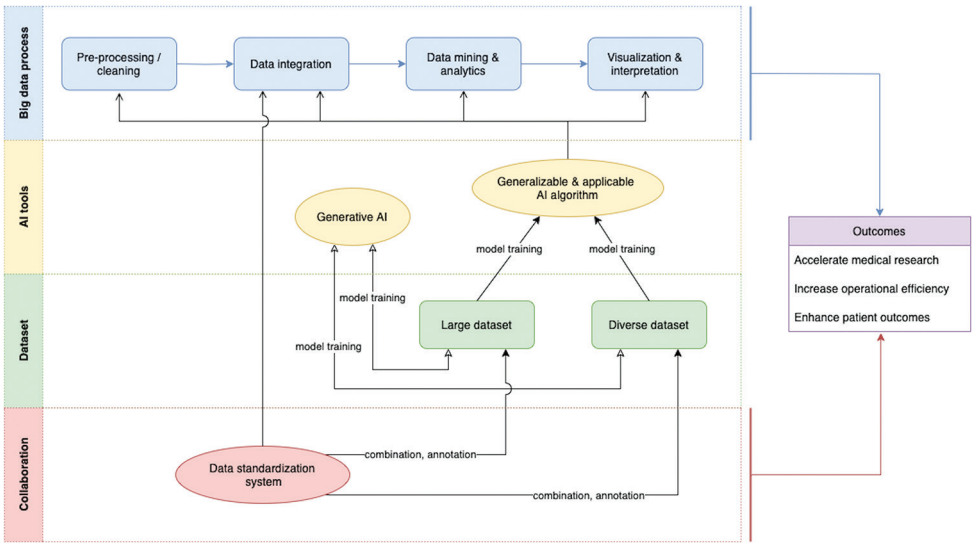

Figure 5: Tools shaping big data in anterior segment imaging. AI = Artificial intelligence

This capability of generative AI can be particularly beneficial in fields like AS imaging, where existing datasets are often scarce and limited in diversity. By generating synthetic images that reflect a wide range of anatomical variations and pathological conditions, generative AI can fill gaps in datasets, providing a richer basis for training diagnostic AI algorithms. Consequently, this leads to more robust and universally applicable AI models, enhancing their accuracy and reliability in clinical settings.

Data standardization system

Addressing the challenges of data integration and scarcity in big data necessitates a collaborative approach across various settings or organizations. When data from multiple sources are pooled together, it mitigates the issue of data scarcity by expanding the volume and diversity of data. However, the data must be uniform and standardized to make it analytically valuable. To achieve this, data standardization is required to transform the data into a structured, coherent, and analytically ready resource in the collaborative environment is important.

One of the systems embodying this principle is the observational medical outcomes partnership (OMOP) common data model (CDM) conducted by the observational health data sciences and informatics (OHDSI) community. The OMOP CDM is instrumental in transforming health-care data into a common format that supports large-scale analytics. Its primary purpose is to organize structured clinical data, such as diagnoses, medications, laboratory results, or administrative claims databases into a standardized framework.[73] Moreover, health level seven fast health-care interoperability resources (HL7 FHIR) is another tool for data standardization, focusing on interoperability and data exchange between healthcare systems. FHIR uses a modular, resource-based approach that integrates extensive use of available standardized vocabularies, facilitating real-time data exchanges and interactions for health-care applications.[74] This ensures that data remain consistent and universally understandable across different health IT systems. In addition, the informatics for integrating biology and the bedside (i2b2) platform also supports data standardization but offers a more flexible model that adapts to the specific needs of biomedical researchers. i2b2 facilitates the integration of clinical research data with healthcare records within a research network, although it is more focused on the research aspect rather than broad clinical data interchanges like FHIR and OMOP.[75] A comparison of these platforms is shown in Table 2.

Although these platforms are not originally designed to handle image data, they can be extended through AI-assisted processes and flexible modeling. Natural language processing algorithms can analyze the language within image reports, such as machine-calculated parameters or other image-related documentation. Image information can be extracted, annotated, or classified and then quantified into structured data. This structured information can then be mapped to the standardized format of OMOP CDM or managed by utilizing extensions in HL7 FHIR. However, the development of standardized terms and vocabularies for AS imaging remains limited. Taking OMOP CDM as an example, it is noteworthy that while some terms for the AS, such as central corneal thickness, have been integrated into the OMOP CDM standard vocabulary,[76] there is still a lack of inclusion for angle-related parameters, which have not been verified or added yet. Proposing the inclusion of these parameters and their concepts to the OHDSI community would initiate their verification and

Table 2: Comparison of data standardization capabilities in health informatics platforms

Feature/aspect	OMOP	i2b2	HL7 FHIR
Primary focus	Observational health data analytics	Clinical research data management	Interoperability and data exchange
Data standardization	Standardized model (OMOP CDM)	Flexible, hierarchical	Modular, resource-based
Interoperability	High within standardized datasets	Limited, mostly within research networks	High, designed for broad interoperability
Key features	Large-scale data analysis, collaborative research	Data discovery, hypothesis generation	Data exchange, API for health-care applications
Implementation complexity	High (due to large datasets and analytics)	Moderate (depends on specific research needs)	Moderate-to-high (due to extensive API features)
Vocabulary/ resource verification	Use common vocabularies; ensures consistent use of standardized vocabularies across datasets through the concept verification process	Flexible use of standard vocabularies, including SNOMED CT, RxNorm, and ICD, dependent on local implementation	Support for validation tools and services to ensure proper use of resource compliance and standardized vocabularies like LOINC, SNOMED CT, RxNorm, and ICD
Image data handling	References to image data; not for direct management or annotation	Can store metadata about images; extended via plugins for better integration	Supports references to images and metadata handling
Extracted image annotations	Can standardize image annotations and detailed image reports through standard vocabularies	Supports extensions for handling specialized data like image annotations and detailed image reports	Supports extensions for handling specialized data like image annotations and detailed image reports

OMOP CDM=Observational medical outcomes partnership common data model, i2b2=Informatics for integrating biology and the bedside, HL7 FHIR=Health level seven fast health-care interoperability resources, API=Application programming interface, LOINC=Logical observation identifiers names and codes, SNOMED CT=Systematized nomenclature of medicine–clinical terms, RxNorm=A standardized nomenclature for clinical drugs, ICD=International Classification of Diseases

integration, increasing the model's usability for further analysis in the glaucoma field.

Conclusions

The integration of AI with AS imaging represents a significant advancement in glaucoma management. The application of ML and DL technologies enables more effective analysis, promoting their adoption in clinical settings. With these powerful tools, clinicians and researchers can enhance patient outcomes more efficiently and automatically. However, while the utilization of AS imaging within big data frameworks shows immense promise, challenges such as data scarcity, standardization and algorithm training remain and require continued efforts to be properly addressed. To fully capitalize on these technological benefits, ongoing innovation and collaborative efforts are essential to navigate the complexities and unlock the full potential of AI-enhanced ophthalmic diagnostics and treatment strategies.

Data availability statement

Data sharing not applicable to this article as no datasets were generated or analyzed during the current study.

Financial support and sponsorship

Nil.

Conflicts of interest

Dr. Shan Lin, an editorial board member at Taiwan Journal of Ophthalmology, had no role in the peer review process of or decision to publish this article. The other authors declared no conflicts of interest in writing this paper.

References

1. Quigley HA, Broman AT. The number of people with glaucoma worldwide in 2010 and 2020. Br J Ophthalmol 2006;90:262-7.
2. Tham YC, Li X, Wong TY, Quigley HA, Aung T, Cheng CY. Global prevalence of glaucoma and projections of glaucoma burden through 2040: A systematic review and meta-analysis. Ophthalmology 2014;121:2081-90.
3. Chansangpetch S, Rojanapongpun P, Lin SC. Anterior segment imaging for angle closure. Am J Ophthalmol 2018;188:xvi-xxix.
4. Varma DK, Simpson SM, Rai AS, Ahmed II. Undetected angle closure in patients with a diagnosis of open-angle glaucoma. Can J Ophthalmol 2017;52:373-8.
5. Radhakrishnan S, Goldsmith J, Huang D, Westphal V, Dueker DK, Rollins AM, *et al*. Comparison of optical coherence tomography and ultrasound biomicroscopy for detection of narrow anterior chamber angles. Arch Ophthalmol 2005;123:1053-9.
6. Wang D, Pekmezci M, Basham RP, He M, Seider MI, Lin SC. Comparison of different modes in optical coherence tomography and ultrasound biomicroscopy in anterior chamber angle assessment. J Glaucoma 2009;18:472-8.
7. Chansangpetch S, Tran B, Perez CI, Siguan-Bell C, Lau K, Nguyen AH, *et al*. Comparison of anterior segment optical coherence tomography parameters among Vietnamese, Chinese, and Whites. Am J Ophthalmol 2018;195:72-82.
8. Chansangpetch S, Nguyen A, Mora M, Badr M, He M, Porco TC, *et al*. Agreement of anterior segment parameters obtained from swept-source fourier-domain and time-domain anterior segment optical coherence tomography. Invest Ophthalmol Vis Sci 2018;59:1554-61.
9. Chansangpetch S, Lin SC. Angle closure glaucoma – Update on treatment paradigms. Curr Ophthalmol Rep 2022;10:63-72.
10. Quek DT, Nongpiur ME, Perera SA, Aung T. Angle imaging: Advances and challenges. Indian J Ophthalmol 2011;59 Suppl: S69-75.
11. Azad RV, Chandra P, Chandra A, Gupta A, Gupta V, Sihota R. Comparative evaluation of RetCam versus gonioscopy images in congenital glaucoma. Indian J Ophthalmol 2014;62:163-6.
12. Panesar A. Machine Learning and AI for Healthcare: Big Data for Improved Health Outcomes. Berkeley, CA: Apress; 2019.
13. Thakur S, Dinh LL, Lavanya R, Quek TC, Liu Y, Cheng CY. Use of artificial intelligence in forecasting glaucoma progression. Taiwan

J Ophthalmol 2023;13:168-83.
14. Rajkomar A, Dean J, Kohane I. Machine learning in medicine. N Engl J Med 2019;380:1347-58.
15. Ittarat M, Cheungpasitporn W, Chansangpetch S. Personalized care in eye health: Exploring opportunities, challenges, and the road ahead for chatbots. J Pers Med 2023;13:1679.
16. Phasuk S, Tantibundhit C, Poopresert P, Yaemsuk A, Suvannachart P, Itthipanichpong R, *et al.* Automated glaucoma screening from retinal fundus image using deep learning. Annu Int Conf IEEE Eng Med Biol Soc 2019;2019:904-7.
17. Bragança CP, Torres JM, Macedo LO, Soares CP. Advancements in glaucoma diagnosis: The role of AI in medical imaging. Diagnostics (Basel) 2024;14:530.
18. Niwas SI, Jakhetiya V, Lin W, Kwoh CK, Sng CC, Aquino MC, *et al.* Complex wavelet based quality assessment for AS-OCT images with application to angle closure glaucoma diagnosis. Comput Methods Programs Biomed 2016;130:13-21.
19. Ouyang J, Mathai TS, Lathrop K, Galeotti J. Accurate tissue interface segmentation via adversarial pre-segmentation of anterior segment OCT images. Biomed Opt Express 2019;10:5291-324.
20. Liu L, Zhai Z, Zhang T, Fan L. Reducing speckle in anterior segment optical coherence tomography images based on a convolutional neural network. Appl Opt 2021;60:10964-74.
21. Li S, Higashita R, Fu H, Li H, Niu J, Liu J, editors. Content-Preserving Diffusion Model for Unsupervised AS-OCT Image Despeckling. Cham: Springer Nature Switzerland; 2023.
22. Jing T, Marziliano P, Wong HT. Automatic detection of Schwalbe's line in the anterior chamber angle of the eye using HD-OCT images. Annu Int Conf IEEE Eng Med Biol Soc 2010;2010:3013-6.
23. Ni Ni S, Tian J, Marziliano P, Wong HT. Anterior chamber angle shape analysis and classification of glaucoma in SS-OCT images. J Ophthalmol 2014;2014:942367.
24. Pham TH, Devalla SK, Ang A, Soh ZD, Thiery AH, Boote C, *et al.* Deep learning algorithms to isolate and quantify the structures of the anterior segment in optical coherence tomography images. Br J Ophthalmol 2021;105:1231-7.
25. Garcia Marin Y, Skrok M, Siedlecki D, Vincent SJ, Collins MJ, Alonso-Caneiro D. Segmentation of anterior segment boundaries in swept source OCT images. Biocybern Biomed Eng 2021;41:903-15.
26. Kao CY, Richdale K, Sinnott LT, Grillott LE, Bailey MD. Semiautomatic extraction algorithm for images of the ciliary muscle. Optom Vis Sci 2011;88:275-89.
27. Wang W, Wang L, Wang T, Wang X, Zhou S, Yang J, *et al.* Automatic localization of the scleral spur using deep learning and ultrasound biomicroscopy. Transl Vis Sci Technol 2021;10:28.
28. Wang W, Wang L, Wang X, Zhou S, Lin S, Yang J. A deep learning system for automatic assessment of anterior chamber angle in ultrasound biomicroscopy images. Transl Vis Sci Technol 2021;10:21.
29. Jiang W, Yan Y, Cheng S, Wan S, Huang L, Zheng H, *et al.* Deep learning-based model for automatic assessment of anterior angle chamber in ultrasound biomicroscopy. Ultrasound Med Biol 2023;49:2497-509.
30. Soh ZD, Tan M, Nongpiur ME, Yu M, Qian C, Tham YC, *et al.* Deep learning-based quantification of anterior segment OCT parameters. Ophthalmol Sci 2024;4:100360.
31. Xu BY, Chiang M, Pardeshi AA, Moghimi S, Varma R. Deep neural network for scleral spur detection in anterior segment OCT images: The Chinese American eye study. Transl Vis Sci Technol 2020;9:18.
32. Liu P, Higashita R, Guo PY, Okamoto K, Li F, Nguyen A, *et al.* Reproducibility of deep learning based scleral spur localisation and anterior chamber angle measurements from anterior segment optical coherence tomography images. Br J Ophthalmol 2023;107:802-8.
33. Bolo K, Apolo Aroca G, Pardeshi AA, Chiang M, Burkemper B, Xie X, *et al.* Automated expert-level scleral spur detection and quantitative biometric analysis on the ANTERION anterior segment OCT system. Br J Ophthalmol 2024;108:702-9.
34. Huang AS, Belghith A, Dastiridou A, Chopra V, Zangwill LM, Weinreb RN. Automated circumferential construction of first-order aqueous humor outflow pathways using spectral-domain optical coherence tomography. J Biomed Opt 2017;22:66010.
35. Peroni A, Paviotti A, Campigotto M, Abegão Pinto L, Cutolo CA, Gong J, *et al.* Semantic segmentation of gonio-photographs via adaptive ROI localisation and uncertainty estimation. BMJ Open Ophthalmol 2021;6:e000898.
36. Fu H, Baskaran M, Xu Y, Lin S, Wong DW, Liu J, *et al.* A deep learning system for automated angle-closure detection in anterior segment optical coherence tomography images. Am J Ophthalmol 2019;203:37-45.
37. Tian J, Marziliano P, Baskaran M, Wong HT, Aung T. Automatic anterior chamber angle assessment for HD-OCT images. IEEE Trans Biomed Eng 2011;58:3242-9.
38. Shan J, DeBoer C, Xu BY. Anterior segment optical coherence tomography: Applications for clinical care and scientific research. Asia Pac J Ophthalmol (Phila) 2019;8:146-57.
39. Xu BY, Friedman DS, Foster PJ, Jiang Y, Porporato N, Pardeshi AA, *et al.* Ocular biometric risk factors for progression of primary angle closure disease: The Zhongshan angle closure prevention trial. Ophthalmology 2022;129:267-75.
40. Xu BY, Friedman DS, Foster PJ, Jiang Y, Pardeshi AA, Jiang Y, *et al.* Anatomic changes and predictors of angle widening after laser peripheral iridotomy: The Zhongshan angle closure prevention trial. Ophthalmology 2021;128:1161-8.
41. Xu Y, Liu J, Tan NM, Lee BH, Wong DW, Baskaran M, *et al.* Anterior chamber angle classification using multiscale histograms of oriented gradients for glaucoma subtype identification. Annu Int Conf IEEE Eng Med Biol Soc 2012;2012:3167-70.
42. Xu Y, Liu J, Cheng J, Lee BH, Wong DW, Baskaran M, *et al.* Automated anterior chamber angle localization and glaucoma type classification in OCT images. Annu Int Conf IEEE Eng Med Biol Soc 2013;2013:7380-3.
43. Fu H, Xu Y, Lin S, Wong DW, Mani B, Mahesh M, *et al.*, editors. Multi-context deep network for angle-closure glaucoma screening in anterior segment OCT. In: Medical Image Computing and Computer Assisted Intervention MICCAI 2018. Cham: Springer International Publishing; 2018.
44. Xu BY, Chiang M, Chaudhary S, Kulkarni S, Pardeshi AA, Varma R. Deep learning classifiers for automated detection of gonioscopic angle closure based on anterior segment OCT images. Am J Ophthalmol 2019;208:273-80.
45. Shi G, Jiang Z, Deng G, Liu G, Zong Y, Jiang C, *et al.* Automatic classification of anterior chamber angle using ultrasound biomicroscopy and deep learning. Transl Vis Sci Technol 2019;8:25.
46. Fu H, Xu Y, Lin S, Wong DW, Baskaran M, Mahesh M, *et al.* Angle-closure detection in anterior segment OCT based on multilevel deep network. IEEE Trans Cybern 2020;50:3358-66.
47. Zheng C, Koh V, Bian F, Li L, Xie X, Wang Z, *et al.* Semi-supervised generative adversarial networks for closed-angle detection on anterior segment optical coherence tomography images: An empirical study with a small training dataset. Ann Transl Med 2021;9:1073.
48. Li F, Yang Y, Sun X, Qiu Z, Zhang S, Tun TA, *et al.* Digital gonioscopy based on three-dimensional anterior-segment OCT: An international multicenter study. Ophthalmology 2022;129:45-53.
49. Porporato N, Tun TA, Baskaran M, Wong DW, Husain R, Fu H, *et al.* Towards 'automated gonioscopy': A deep learning algorithm for 360 angle assessment by swept-source optical coherence tomography. Br J Ophthalmol 2022;106:1387-92.
50. Hao J, Fu H, Xu Y, Hu Y, Li F, Zhang X, *et al.*, editors. Reconstruction and quantification of 3D iris surface for angle-closure glaucoma

detection in anterior segment OCT. In: Medical Image Computing and Computer Assisted Intervention MICCAI 2020. Cham: Springer International Publishing; 2020.
51. Randhawa J, Chiang M, Porporato N, Pardeshi AA, Dredge J, Apolo Aroca G, *et al.* Generalisability and performance of an OCT-based deep learning classifier for community-based and hospital-based detection of gonioscopic angle closure. Br J Ophthalmol 2023;107:511-7.
52. Fu H, Xu Y, Lin S, Zhang X, Wong DW, Liu J, *et al.* Segmentation and quantification for angle-closure glaucoma assessment in anterior segment OCT. IEEE Trans Med Imaging 2017;36:1930-8.
53. Cheng J, Liu J, Lee BH, Wong DW, Yin F, Aung T, *et al.* Closed angle glaucoma detection in RetCam images. Annu Int Conf IEEE Eng Med Biol Soc 2010;2010:4096-9.
54. Baskaran M, Cheng J, Perera SA, Tun TA, Liu J, Aung T. Automated analysis of angle closure from anterior chamber angle images. Invest Ophthalmol Vis Sci 2014;55:7669-73.
55. Chiang M, Guth D, Pardeshi AA, Randhawa J, Shen A, Shan M, *et al*. Glaucoma expert-level detection of angle closure in goniophotographs with convolutional neural networks: The Chinese American eye study. Am J Ophthalmol 2021;226:100-7.
56. Hao L, Hu Y, Xu Y, Fu H, Miao H, Zheng C, *et al.* Dynamic analysis of iris changes and a deep learning system for automated angle-closure classification based on AS-OCT videos. Eye Vis (Lond) 2022;9:41.
57. Seager FE, Jefferys JL, Quigley HA. Comparison of dynamic changes in anterior ocular structures examined with anterior segment optical coherence tomography in a cohort of various origins. Invest Ophthalmol Vis Sci 2014;55:1672-83.
58. Zhou Q, Guo J, Chen Z, Chen W, Deng C, Yu T, *et al.* Deep learning-based classification of the anterior chamber angle in glaucoma gonioscopy. Biomed Opt Express 2022;13:4668-83.
59. Bai X, Niwas SI, Lin W, Ju BF, Kwoh CK, Wang L, *et al.* Learning ECOC code matrix for multiclass classification with application to glaucoma diagnosis. J Med Syst 2016;40:78.
60. Niwas SI, Lin W, Bai X, Kwoh CK, Jay Kuo CC, Sng CC, *et al.* Automated anterior segment OCT image analysis for angle closure glaucoma mechanisms classification. Comput Methods Programs Biomed 2016;130:65-75.
61. Niwas SI, Lin W, Bai X, Kwoh CK, Sng CC, Aquino MC, *et al.* Reliable feature selection for automated angle closure glaucoma mechanism detection. J Med Syst 2015;39:21.
62. Niwas SI, Lin W, Kwoh CK, Kuo CC, Sng CC, Aquino MC, *et al.* Cross-examination for angle-closure glaucoma feature detection. IEEE J Biomed Health Inform 2016;20:343-54.
63. Wanichwecharungruang B, Kaothanthong N, Pattanapongpaiboon W, Chantangphol P, Seresirikachorn K, Srisuwanporn C, *et al.* Deep learning for anterior segment optical coherence tomography to predict the presence of plateau Iris. Transl Vis Sci Technol 2021;10:7.
64. Hao H, Zhao Y, Yan Q, Higashita R, Zhang J, Zhao Y, *et al.* Angle-closure assessment in anterior segment OCT images via deep learning. Med Image Anal 2021;69:101956.
65. Hao J, Li F, Hao H, Fu H, Xu Y, Higashita R, *et al.* Hybrid variation-aware network for angle-closure assessment in AS-OCT. IEEE Trans Med Imaging 2022;41:254-65.
66. Koh V, Swamidoss IN, Aquino MC, Chew PT, Sng C. Novel automated approach to predict the outcome of laser peripheral iridotomy for primary angle closure suspect eyes using anterior segment optical coherence tomography. J Med Syst 2018;42:107.
67. Wang T, Zhong L, Yuan J, Wang T, Yin S, Sun Y, *et al.* Quantitative analysis of functional filtering bleb size using Mask R-CNN. Ann Transl Med 2020;8:709.
68. Mastropasqua L, Agnifili L, Brescia L, Figus M, Posarelli C, Oddone F, *et al*. A deep learning approach to investigate the filtration bleb functionality after glaucoma surgery: A preliminary study. Graefes Arch Clin Exp Ophthalmol 2024;262:149-60.
69. Grand Challenge for Medical Image Analysis. DRIVE: Digital Retinal Images for Vessel Extraction: Grand Challenge; 2019. Available from: https://www.drive.grand-challenge.org/DRIVE/. [Last accessed on 2024 May 05].
70. Fumero Batista FJ, Diaz-Aleman T, Sigut J, Alayon S, Arnay R, Angel-Pereira D. RIM-ONE DL: A unified retinal image database for assessing glaucoma using deep learning. Image Anal Stereol 2020;39:161-7.
71. Zhang Z, Yin FS, Liu J, Wong WK, Tan NM, Lee BH, *et al.* ORIGA(-light): An online retinal fundus image database for glaucoma analysis and research. Annu Int Conf IEEE Eng Med Biol Soc 2010;2010:3065-8.
72. Fu H, Li F, Orlando JI, Bogunović H, Sun X, Liao J, *et al*. REFUGE: Retinal Fundus Glaucoma Challenge:IEEE Dataport; 2019. [doi: 10.21227/tz6e-r977].
73. OHDSI. The Book of OHDSI: Observational Health Data Sciences and Informatics. New York, NY: OHDSI; 2019.
74. Health Level Seven International. Health Level Seven Fast Healthcare Interoperability Resources: HL7; 2023. Available from: https://www.hl7.org/fhir/. [Last accessed on 2024 May 05].
75. The i2b2 tranSMART Foundation. i2b2: Informatics for Integrating Biology and the Bedside; 2024. Available from: https://www.i2b2.org. [Last accessed on 2024 May 05].
76. ATHENA. OHDSI Vocabularies Repository: Odysseus Data Services; 2024. Available from: https://www.athena.ohdsi.org. [Last accessed on 2024 May 05].